SOLAR INTERFEROMETRY: A REVOLUTIONARY CONCEPT FOR HIGH RESOLUTION SOLAR PHYSICS

L. Damé, M. Hersé, M. Kozlowski, M. Martić, M. Merdjane
Service d'Aéronomie du CNRS, BP 3, 91371 Verrières-le-Buisson Cedex, France
Phone: +33-1-64474328, Fax: +33-1-69202999, e-mail: luc.dame@aerov.jussieu.fr
web: http://must.aerov.jussieu.fr

J. Moity
DASOP, Observatoire de Meudon, 92195 Meudon, France

ABSTRACT

Following several years of design studies of UV imaging interferometers for Solar Physics Space Missions (SIMURIS/SUN–MUST–SOLARNET), we decided, in 1995, for demonstration purpose, to realize a complete test of the cophasing feasibility and performance directly on the Sun. Accordingly, our laboratory breadboard of a 2-Telescope cophased interferometer (on which demonstration of the cophasing method were performed from 1992 to May 1995) was moved to the "Grand Sidérostat de Foucault" at Meudon Observatory. During summer 1995, and up to March 1997, the feasibility and performances of the cophasing of two telescopes on extended objects like the Sun, the Moon and planets (Mars, Saturn, Jupiter) were demonstrated. These results really open the possibility to use and discover from solar interferometers, not only in Space but also on ground. With a 1 meter baseline or so, a ground imaging interferometer (e.g. THEMIS with a phased pupil) will reach a PERMANENT spatial resolution of 0.1" on a coherent field-of-view of 40", allowing to untangle the confining and dissipating mechanisms and processes in magnetic flux tubes, prominences, flares, *etc*. This factor 10 in resolution is a factor 100 in flux concentration, i.e. a major gain for MAGNETIC FIELDS and POLARIZATION measurements too. We describe progress in designing Solar Interferometers in Space and on ground and a possible adaptation of the interferometry techniques to THEMIS.

1. INTRODUCTION

Since the *Solar Ultraviolet Network* (SUN) proposed to ESA in 1989 (Damé et al., 1989, Coradini et al., 1991), we have developed an instantaneous direct imaging interferometry concept based on a compact interferometer configuration (several telescopes, 3 to 5, on a circular baseline, but large enough compared to the baseline so that the spatial frequencies plane is filled). It was proposed to ESA as a satellite mission in 93 (*Multi-mirror Ultraviolet Solar Telescope*, MUST/SIMURIS proposal, Damé et al., 1993a) and, more recently, April 15, 1997, as an Externally Mounted Payload on the International Space Station (Solar and Planetary High Resolution UV Imaging by Interferometry, SOLARNET, Damé et al., 1997). In support to ESA studies, CNES engaged in 92 Research and Technologies (R & T) funds for the realization of a 2-Telescope Breadboard to demonstrate the heart of the system: the measurement of an absolute phase and the cophasing control of the interferometer.

The breadboard was completed in spring 1994 and by September 1994 a complete laboratory demonstration of the cophasing of two-telescopes on extended objects was achieved with remarkable performances. During summer 1995 the breadboard was installed at Meudon Observatory at the “Grand Sidérostat de Foucault” and the first direct cophasing on the Sun was made with a phase control of $\lambda/140$. These cophasing experiments were repeated in 1996 and better performances were achieved ($\lambda/240$). Following these successes we can now sustain that we have the recipe and the cooking skills for the realization of a major instrument for the advance of Solar Physics at the beginning of next century: the Solar Interferometer, either on ground (MACS: *Multi-Aperture Cophased System*) or in Space (SOLARNET).

In the following, we briefly recall the objectives and concepts of a ground Solar Interferometer, explain the constraints imposed by the measurement of a phase over extended objects, present the laboratory and sky results obtained with the first solar interferometric experiment of cophasing on extended objects (Sun and Planets), and indicate the next step of the demonstration programme on the breadboard: a 3-Telescope cophased (active cophasing) and pointed (active pointing) Imaging Interferometer for the Sun and planets. We conclude on the possible adaptation of these techniques — MACS Techniques — to THEMIS.

2. SCIENTIFIC OBJECTIVES FOR HIGH RESOLUTION

The relevant minimum observable scale in the solar atmosphere may be of the order of 10–30 km since smaller scales will probably be smeared out by plasma micro-instabilities (such as drift waves). This scale range is comparable to — though slightly smaller — the photon mean free path in the chromosphere (~ 60–70 km). Slightly larger scales can be expected in the corona (though gradient across coronal loops may also be a few km). Altogether this situation is rather fortunate because we have access to higher resolutions in the far UV than in the visible and X-rays (multilayer telescopes are limited to resolutions of 1 arcsec or so). In the UV, the emission lines are generally thin, i.e. not affected by the optically thick transfer conditions which prevail in the visible and near UV lines accessible from ground, and we can expect to see structures with scales 10 to 30 km. In the visible, thick transfer in the atmosphere blurs the signature of structures and nothing smaller than 70–100 km should be observed. This is, indeed, well delineating the maximum useful scientific spatial resolution. This means that with a single instrument of meter class diameter we have the appropriate, *scientifically justified*, spatial resolution for both the UV (20 km at Lyman Alpha 121.6 nm) and the visible (60 km in the Ca II K line 396.3 nm). More details on the scientific objectives in the UV and FUV can be found Damé et al. (1993b). For the visible, most of the THEMIS literature could be cited since the 0.1" is the observing objective of all programs.

The breakthrough in high spatial resolution observations (10 times more resolution, 100 times more flux in fine structures if they are of 0.1" in size) will allow to study the coupling between turbulent convective eddies and magnetic fields in the photosphere, fibrils and their chromospheric connections, network bright points and their coupling to waves and magnetic fields, *etc*. Also of prime interest are the plasma heating processes and thermal inputs of flares and microflares and their fine magnetic field structures.

3. WHY AN INTERFEROMETER?

If the need for high spatial and spectral resolutions is commonly agreed, the question left is why an interferometer and not a single-dish large telescope? The answer is that the required measurement needs exceed conventional instrumentation limitations. A 1 m telescope diffraction-limited is difficult to construct even in the visible (THEMIS does not escape this situation). And, even assuming that such a perfect 1 m telescope could be built, it would be extremely costly to control its stability because of the primary figure evolution but also of the large secondary and critical primary–secondary alignments and distance control.

The Michelson interferometric approach represents significant advantages over direct diffraction-limited large telescope imaging. Only small telescopes (or subpupils of a main pupil) are necessary and active pointing of the telescopes can be made directly on the secondary of each of the small telescopes (or on a small active mirror afterwards). Small telescopes or segments of a large telescope like THEMIS can possess a perfect — or near perfect — figure and reach their diffraction limit. Interferometry requires to control the residual optical path delays between telescopes but this, consequently, guarantees a perfect output wavefront suitable for diffraction-limited imaging.

Adaptive optics is not an alternative to obtain the correct figure precision of large mirrors or to control the resulting errors, because of thermal cycling but also (on ground) of the mechanical deformations due to their weight. Note that aligning a segmented mirror requires 6 degrees of

freedom and a control of the distance between the primary and secondary mirrors. This very complex control loop is not required with an interferometer made of small telescopes or when working on a limited set of pupil's segments (beside fine pointing needs, only one degree of freedom is required: the phase control).

Altogether, the modest baseline required to obtain major scientific results and the simplified control of an imaging interferometer (which doesn't need an absolute metrology like astrometric programs) result in a very reasonable optical complexity and cost which open solar interferometry programs to the medium size satellites programs, to the accommodation possibilities of the International Space Station, but also to large ground telescopes like THEMIS.

4. DESIGN OF A SOLAR INTERFEROMETER

To study the ultimate fine structure of the Sun, a solar interferometer needs to image an extended field-of-view (FOV) covered with complex structures. And, since many structures of interest are evolving rapidly (in a few seconds or even less), this imaging cannot be achieved by classical long-baseline interferometry techniques where fringes' visibilities are measured sequentially.

These constraints (FOV and time resolution) prompt to design an interferometer with instantaneous imaging capability i.e., first, to the choice of a compact array. By compact is meant that the spatial frequency coverage of the array is comparable to a single dish telescope in one fundamental aspect: complete coverage of spatial frequencies, i.e. there are no zeroes in the modulation transfer function of the array (cf. Fig. 1). Image restoration is, in this case, based on a direct deconvolution. A central issue for interferometric imaging is, therefore, a proper (i.e. compact) configuration of the array.

The other important requirement is to control the residual optical path delays between the different telescopes to a fraction of a wavelength, i.e. to *cophase* the interferometer. This allows all the recorded fringes to be used *instantaneously*, since not affected by a significant phase problem (thus allowing a robust image reconstruction approach). The consequence of importance brought by this cophased approach is that, permanently, we have the insurance of a near perfect wavefront (stable transfer function), the telescopes of the array being controlled to their optimum phase position.

This complete spatial frequencies coverage is the basic difference between classical two-telescope interferometers and compact multi-telescopes interferometers. In the two-telescopes case, the fringes do contain high resolution information even though most of the spatial frequencies are lacking between the low frequencies — due to the area of the small telescopes' primaries — and a high resolution peak due to the pair of telescopes. The data analysis then relies, first, on a measurement of the fringes' visibilities at these specific spatial frequencies, second, on a sampling of the other spatial frequencies (e.g. by moving the telescopes) and, third, on an image reconstruction from these data.

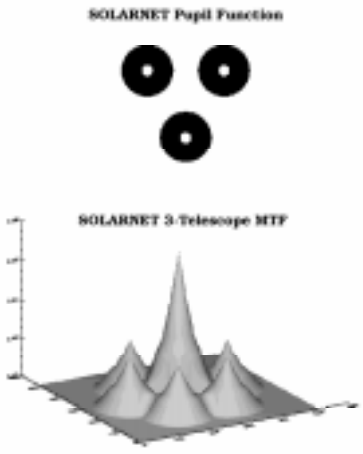

Fig. 1 - SOLARNET configuration (3 x Ø35 cm telescopes on a 95 cm baseline) and MTF.

In a compact multi-telescopes case, all the spatial frequencies are included in the image formed, but their relative weighting is not as smooth as in the single dish case (cf. Fig. 1). However, the absence of zeroes enables stable image restoration with direct deconvolution algorithms which, in practice, simply reweight properly the spatial frequencies.

In this approach, *images* (i.e. extended FOV's) are recorded and restored without the intermediate steps of fringes' visibility measurement, u,v plane sampling and painful image reconstruc-

tion, necessary when diluted interferometric arrays are considered. Further, since the number of phase relations is very large, the FOV is important (40 arcsec) while a diluted array of a few telescopes would have a FOV of 5 x 5 pixels or so... Then, a multi-telescopes compact interferometer has equivalent imaging capabilities than a classical telescope.

5. PHASE CONTROL AND COHERENCE

The major conceptual choice of our interferometric approach is to cophase the array. By cophase we mean real-time control of the phase differences between the telescopes (or pupil's segments), i.e. constant monitoring of the equality of the optical path-lengths traveled by the different beams. By this mean, the transfer function, although still rather poor (cf. Fig. 1), is stable. Cophasing has a sound justification since only cophased arrays can integrate light, i.e. benefit from long exposures and, thus, from better signal to noise ratios. The result is a significant increase in the complexity and dynamic range with which images can be reconstructed. Numerous simulations have been performed (Damé, 1994, Damé and Martic, 1992) to demonstrate that such cophased arrays can properly observe complex and extended objects. It was shown that, at a given wavelength, $\lambda/10$ of phase stability guarantees that near perfect image reconstruction can be achieved. This capability requires a specific cophasing control – using reference interferometers – which we have been studying for several years (see, e.g., Damé, 1992, 1993). The measurement of an absolute phase on an extended object is not straightforward and we will first recall some basic notions of coherence.

5.1 Reminders

"Cophasing" two or more telescopes supposes a minimum of knowledge of our method of phase control. In order to be as much as possible understandable in what we are doing and the tests that were carried we present some reminders, first on coherence and, then, on the Double Synchronous Detection Method.

5.1.1 Coherence

When the light of a source is not monochromatic, from the knowledge its spectrum we can calculate the mutual coherence function Γ:

$$\Gamma(\mathbf{u_1}, \mathbf{u_2}, \tau) = \int_0^\infty e^{-2\pi i \nu \tau} d\nu$$

where ν is the frequency and τ the retardation time. The mutual coherence function has the dimensions of intensity. From it can be defined the dimensionless degree of coherence γ:

$$\gamma(\mathbf{u}_1, \mathbf{u}_2, \tau) = \frac{\Gamma(\mathbf{u}_1, \mathbf{u}_2, \tau)}{\sqrt{I(\mathbf{u}_1)\, I(\mathbf{u}_2)}}$$

It is the direct observable quantity of optics, being measured by simple interference, e.g. in the Mach-Zehnder set up which we used for our demonstrations of cophasing. We have both the *addition* interferogram and the *subtracted* interferogram, with a phase difference of between the signals; the interferogram can be subtracted from the background, and therefore we can separate interferogram and background in low visibility cases.

When the source is extended and when the light is not monochromatic, temporal effects are combined with spatial effects and what is to be considered is the result integrated over an extended source ζ of spectral irradiance $E(\mathbf{x},\nu)$. The coherence function in this more general case is given by (for an explanation of the notations see Fig. 3):

$$\Gamma(\vec{\mathbf{u}}_1, \vec{\mathbf{u}}_2, \tau) = \int_0^\infty e^{-2\pi i \nu \tau} d\nu \int_\varsigma \frac{E(\vec{\mathbf{x}}, \nu) e^{2\pi i \nu (R_2 - R_1)/c} d\vec{\mathbf{x}}}{R_1 R_2} \qquad [1]$$

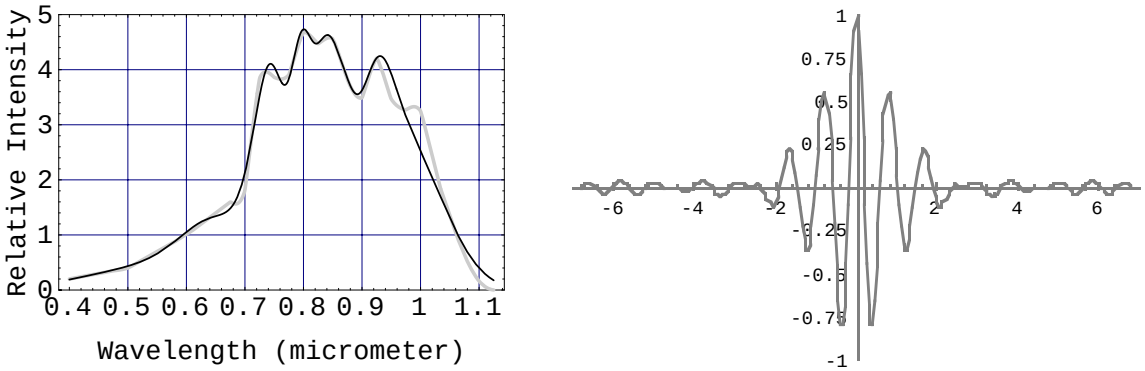

Fig. 2 - Visibility as a function of the optical path delay (in µm) for an ideal white light source (point source with the spectrum shown left). Note that we have "only" 5 fringes on ± 2 µm

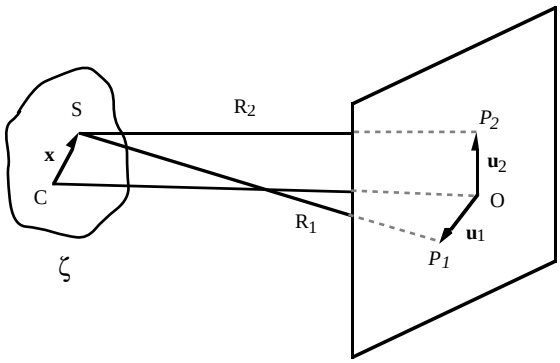

Fig. 3 - Notation for the mutual coherence function.

With the usual approximation for path difference (i.e. that variations in path differences are caused only by either **u** or **x** changing from zero, which implies that the imaging system is perfect, converting a spherical wave at the entrance pupil to a spherical wave of different curvature at its exit pupil), this becomes a three-dimensional Fourier transform. In other words, the coherence volume which has for base the coherence area and height $c\tau$, is connected by an uncertainty relation with the volume in reciprocal space, defined by the product of the solid angle subtended by the source and its bandwidth.

We have formally evaluated the integral [1] for a white light source (whose spectrum is shown on Fig. 2: ~ 300 nm FWHM centered at 850 nm) of different source sizes (diameter) for a reference interferometer which interbaseline (distance between two telecopes center to center) is 1.5 time the telescope diameter:

a) S = 0.3"
b) S = 0.5"
c) S = 0.6"
d) S = 0.8"
e) S = 1"

This is assuming that the source is uniform (and, in this case, that the telescope has a 20 cm diameter; results are indeed the same for smaller sources and larger telescopes — inversely proportional — as long as the relation interbaseline to diameter is the same, i.e. a 1.5 time relation).

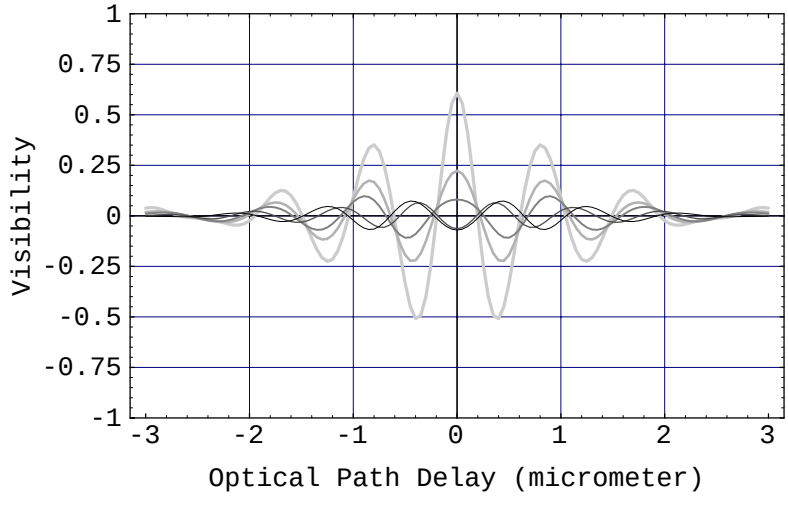

Fig. 4 — Fringes visibility as a function of the Optical Path Delay for a circular configuration in which the interbaselines (distance center to center of the telescopes) are 1.5 time the telescope diameter. Illustration for sources of diameter 0.3", 0.5", 0.6", 0.8" and 1". Curves go from light gray, 0.3", to black, 1" and telescopes of 20 cm (same for sources half size and telescopes 40 cm for example). Interesting to note is that the contrast inversion of the central fringe happens near the interbaseline resolution (as one could expect since the source is resolved).

However, in more realistic cases, the extended source can be arbitrary and, in particular, it can be a double source (e.g. a double star). We have illustrated this on Fig. 5.

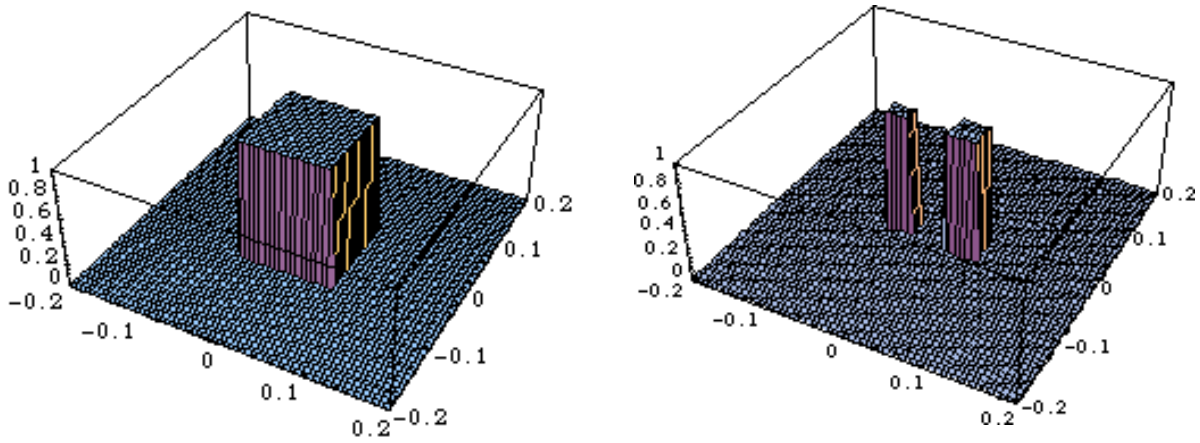

Fig. 5 - Explanation of the uniform and complex source definitions. The source (left) is extended and uniform. The source (right) is also extended but complex (e.g. a double star with one star brighter than the other).

What can be seen from calculations (cf. Fig. 6) is that for very small uniform but extended sources, e.g. 0.12 arcsec (case **A**), the contrast of the central fringe is, indeed, slightly reduced (> 80%) but isn't affected by any phase shift. Larger sources (e.g. 0.36") reduce even more the contrast (~ 40%) but yet without phase shift. By controlling the position of the central fringe, the cophasing is ensured. Though, if the source is highly structured (double source case), an important shift of the central fringe may happen on "large" reference sources (case **B**). Problem with sources 0.36" with 30 cm interbaseline will occur at 0.18" if the interbaseline is 60 cm...

In the case of "real" interferometers (looking for "real reference sources" for cophasing) there are, therefore, less problems to be anticipated with small (and equal) interbaselines even if the reference sources are extended or complex. Because our configurations are compact, we are always in the most favorable case where the interbaselines are the same and small (only 1.5 x the telescope's diameter). For THEMIS (cf. #8, Fig. 15) the situation would be even more favorable since the interbaseline distances are the same as the width of the pupil's segments.

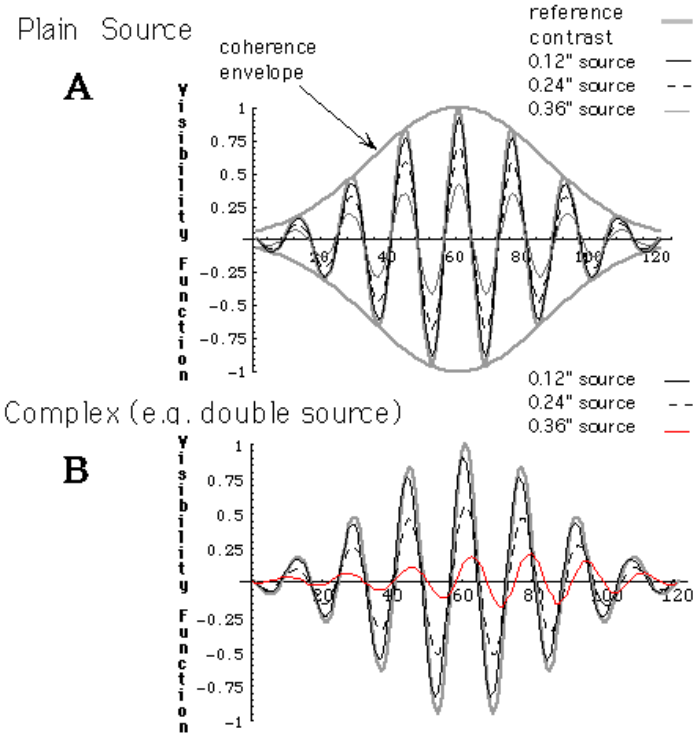

Fig. 6 - "Plain" and "Complex" sources (as defined in Fig. 5) visibility functions for different source extensions from 0.12 to 0.36" (again for a 1.5 ratio interbaseline to diameter of the telescope and a nominal 20 cm telescope). Note that problems occur only when the source is highly complex (such high contrast on structures 0.03" in size are not expected on the Sun, at least in the visible and on a large spectrum) or when the reference field of view transmitted to the cophasing is somehow larger than half the Airy disk of a telescope (possible error larger than λ/100).

5.1.2 Double Synchronous Detection Method

Service d'Aéronomie has a long-standing expertise in white-fringe acquisition and stabilization (cophasing). The method, based on Zero-OPD detection by servo-control on the central white-fringe through synchronous demodulation, has been studied in details and its performances assessed both in laboratory experiments (Damé, 1994, Damé et al., 1994, 1995b), and on the sky, on stars, e.g. on Altair with λ/225 phase stability, and on the Sun, with λ/140 measured phase stability (Damé et al., 1995a, 1995b). The method was further refined in 96 during a new observational campaign at Meudon Observatory where the 2-Telescope breadboard was cophased on a limited selection of stars, Jupiter, Mars, the Moon and on different solar structures. It is worth recalling that the method is an absolute OPD method which provides calibrated fringes amplitude by the use — while the fringe position is servo-controlled by the error signal of a first synchronous demodulation — of a second synchronous demodulation at twice the reference frequency.

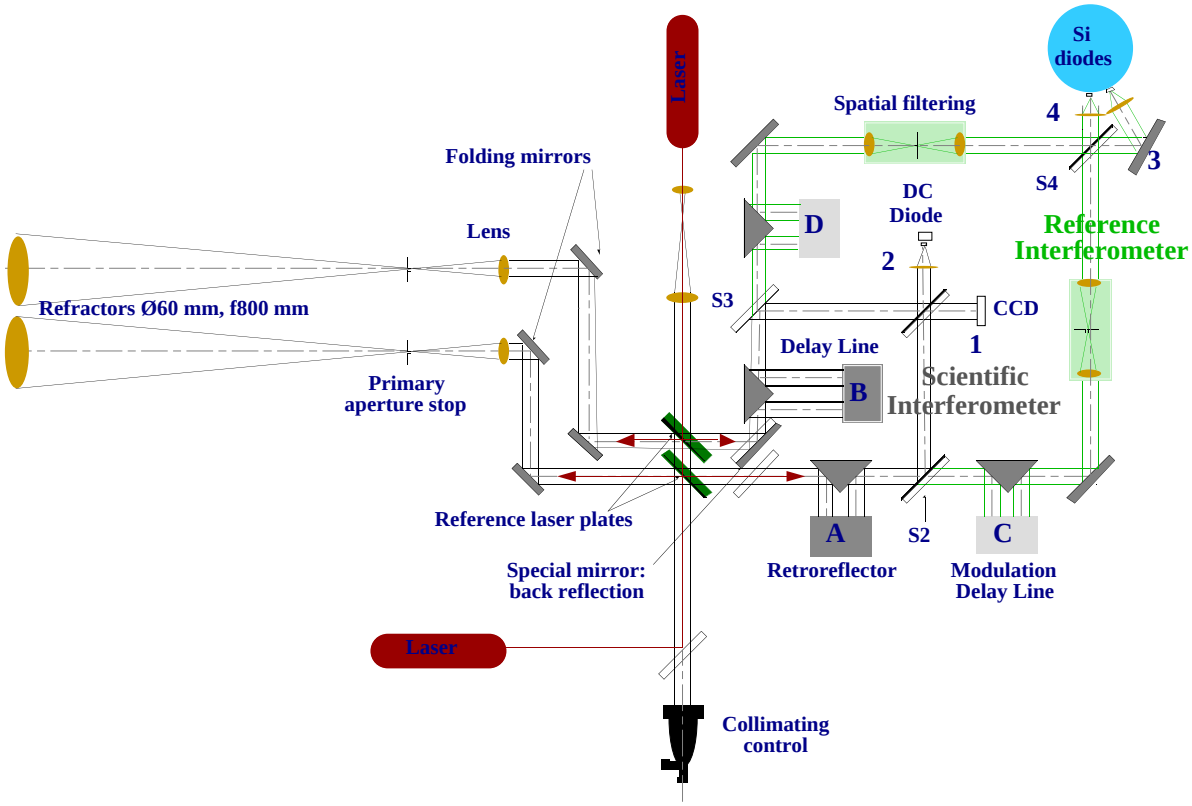

Fig. 7 - Schematic of the laboratory and sky setup used to validate the fringes acquisition and stabilization on the central fringe.

In the Scientific Interferometer (cf. Fig. 7), the delay line "B" is moved up to the region where a signal is detected by a first synchronous detection (a modulation is introduced in the Reference Interferometer by another delay line: "C"). Then, a second synchronous detection, at twice the frequency, measures the amplitude of the signal while the first synchronous detection is active. By this mean, and since the first synchonous detection is active (we are stabilized on the submit of the fringe then), the **amplitude of the fringe is directly measured**.

Fig. 8 explains the principle and Fig. 9 illustrates a practical acquisition and cophasing control on the central fringe made in May 1996 (laboratory measurement). On Fig 9, which displays the synchronous detection signal (i.e. the fringe signal multiplied by a sinus), one can clearly see that the observed signal is very near the theoretical one (cf. Fig. 8). Crosses indicate the measurements made by the synchronous detection at double the frequency while the servo-control is active stabilizing the optical path between the telescopes using whatever fringe providing a signal (even less than 1% contrast: see for example Table 1, Damé, 1996). Jumping from fringe to fringe we are, then, able to determine the largest one, i.e. the central one.

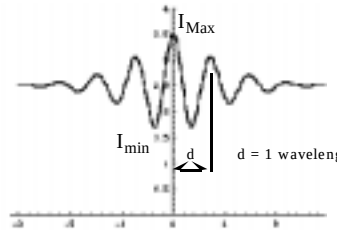

Temporal Coherence Fringes as seen by their Intensity

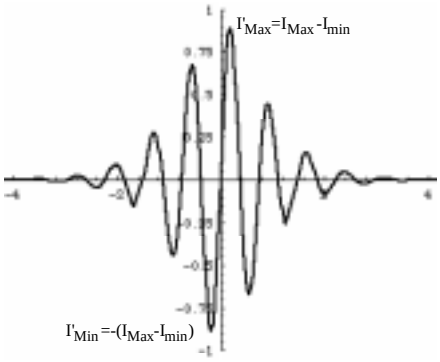

Illustration of the Synchronous Demodulation Signal obtained at the Modulation Frequency (Simulated by Multiplying the Fringes Signal with a Sin at the Frequency of the Reference Path-Length Modulation)

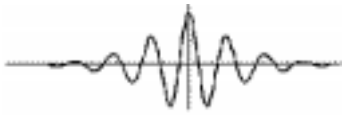

Illustration of the Synchronous Demodulation Signal Obtained at **twice** the Modulation Frequency → Similar to the Fringes Pattern

Fig. 8 - Fringes, Synchronous Detection and Synchronous Detection at twice the reference frequency.

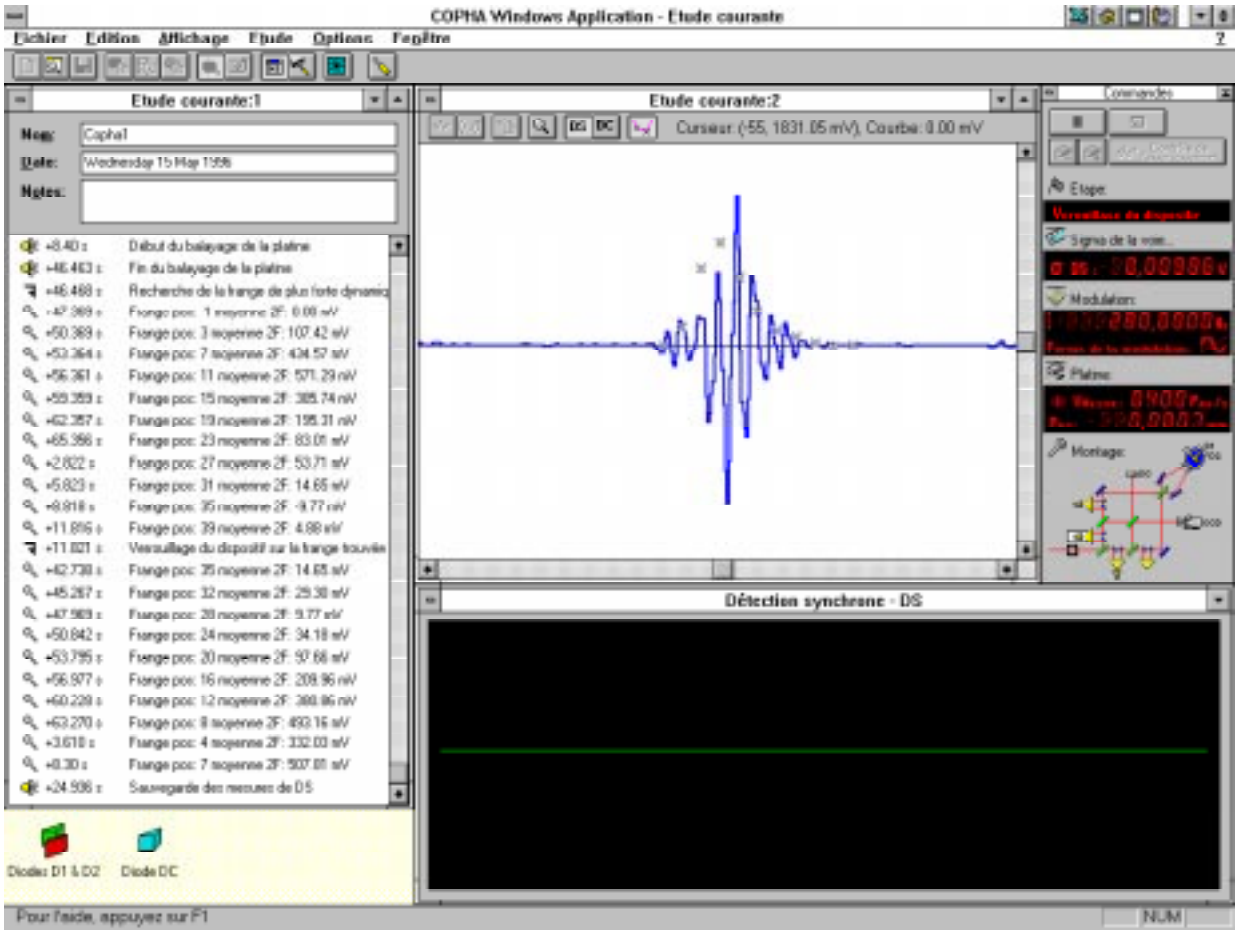

Fig. 9 - Synchronous Detection signature of the fringes as observed during an acquisition.

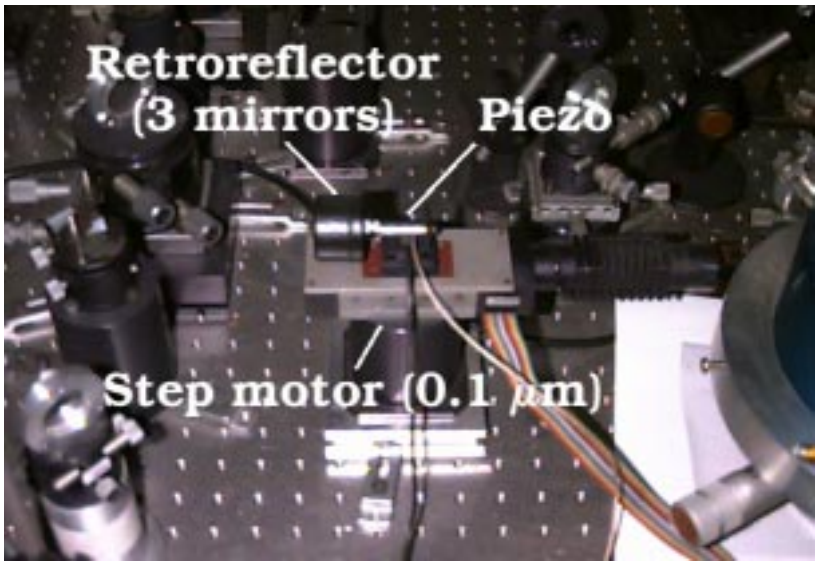

Fig. 10 - Current Delay Line implementation on the 2-Telescope Solar Interferometer Breadboard at the Observatory of Meudon (March 1997). The Delay Line consists in a retroreflector (3 assembled mirrors), a step motor (Micro-Contrôle, course 20 mm, elementary steps of 0.1 μm) and a piezoelectric ceramic (± 7 μm).

Table 1. Comparison of theoretical and observed contrasts (extremum – positive or negative – not necessarily corresponding to the central fringe value), and the corresponding cophasing stabilities that were achieved.

Field-of-view (as a fraction of telescope Airy disk)	Experimental field stop (μm)	Theoretical contrast (%)	Observed contrast (%)	σ of residual fluctuations (nm)	Achieved stabilities ($\lambda_{ref.}$ = 550 nm)
1/3	5	70.4	74.6	3	λ/300
1/2	10	-19.5	-18.9	5	λ/180
1	15	6.7	5.2	7	λ/130
1 1/4	20	2.7	3.5	—	—
1 1/2	25	-3.1	-3.6	—	—
2	30	3.1	3.2	7	λ/130
3	50	-1.3	-0.8	9	λ/100

The acquisition process is such that we first pass over the fringes when we have detected them and record the intensities measured (see the "Journal: Etude courante" on Fig. 9 which reflects that). Then we back up to the first detectable fringe and put the servo on (i.e. the piezoelectric ceramic on the delay line retroreflector is fed — cf. illustration, Fig. 7 — by the synchronous detection error signal). At this time we are on the submit of a fringe and we measure, via the second synchronous detection, the amplitude of that fringe. When this is done, we cut the servo and "jump" to the next fringe using the first stage of the delay line (the step motor). Because of the very large spectral bandpass that we use (300 nm), we always have more or less 5 fringes on ± 2 μm, fringes at 0.8 μm one from each other, i.e. 4 steps (at 2 x 0.1 μm) of the delay line. When the "jump" is made, the servo is put back on which leads us to the submit of the next fringe. And, when we are there, and stabilized, we measure the amplitude by the synchronous detection at double the frequency. These "jumps" are reflected in the "Journal: Etude courante" again and, when the intensity lowers rather than improving, then we back one step and are on the central fringe. A comparison with the side values and with the values of the initial scan confirms or not that the process has been successful. This is simple and efficient. With a limited number of fringes (which is a definite flux advantage since the spectral bandpass is larger) the identification process, even when contrasts are as low as 1%, has never failed. Only when numerous fringes are considered is the identification more difficult since fringes have almost the same amplitude. As reported in Table 1, very high stabilities were achieved by this method (λ/100) and, for extended, Sun-like objects, with better results when using small flux/high contrast (small holes) rather than larger flux/low contrast (large holes to the interbaseline resolution).

Important to this process of acquisition and stabilization is, indeed, the control software and the acquisition card beside the "pure" hardware: diode amplifiers, synchronous detections, frequency generator, piezoelectrics, step motors, *etc*. Since 1994, we developed and use a dedicated C++ program (20 000 lines of code) to perform, under Windows 3.11 (using the multimedia — video — clock) this real-time process of acquisition and stabilization at the 300 Hz rate of the modulation (sampling at 3 KHz). With the need to control not only one but several interferometers simultaneously we have developed a new software (still in C++ and Visual Basic) but this time under a "real" multitasking and multithreading preemptive system, Windows NT 4.0. This has a definite advantage in terms of response and control of the tasks since the control to the instruments (the GPIB/IEEE link) is faster with a very limited risk of collisions and since, moreover, all the internal tasks of acquisition or fringe jumps can be programmed as independent "threads" in the program. Beside the evident gain in terms of multi-telescopes / interferometers control and real-time capacities, better stability performance is also expected since, in addition, a new and faster (500 Ksamples/s) acquisition card has been provisioned allowing gain adjustments on the different entry channels (overcoming the noise/dynamic problem encountered with the present card). This new acquisition software (and hardware) will be used by mid-May 1997 on the 3-Telescope Imaging Breadboard. With this system we will truly enter the world of controlled interferometric imaging.

6. THE 2-TELESCOPE BREADBOARD AT MEUDON

Although the laboratory results obtained in 1994 (cf. Table 1) were excellent and hardly contestable, they were still doubts that the laboratory conditions could reproduce without bias the exact solar conditions. Since the cophasing is performed in the visible, either in the Space Instruments or in the ground programme, we therefore moved the whole experiment to the “Grand Sidérostat de Foucault” at Meudon Observatory from May to July 1995 for a complete demonstration of the cophasing on the Sun and obtained the first solar directly cophased interferometric fringes with independent telescopes (cf. Damé, 1995b and 1996). Our major problem was the lack of pointing control (no reference of the refractors' position) since, despite the double laser metrology and the autocollimating lens (cf. Fig. 7), only alignments from the field stops to the interferometers could be mastered (but well mastered: the two lasers being aligned, the two interferometers are aligned up to the selection holes right at the focus of the refractors). However, if an objective moves, the solar image moves and the fields do not overlap anymore (selecting holes are a few µm) resulting in no interferences. Because of that situation, pre-alignment was made, first, with a collimating mirror in front of the objectives and, second, by the use of a perfect point source: a star. We observed at night Arcturus and Altair (for this we controlled the speed of the siderostat motor by a frequency variator) and during the night of July 6, we aligned and then cophased our interferometer on Altair with a measured stability of $\lambda/225$ but a limited contrast (40%). At 7:00 AM the 7th, we cophased the interferometer on the Sun using a 10 µm hole. We measured a fairly low contrast of 4 % but nevertheless achieved a stability of $\lambda/140$ (at $\lambda_{ref.} = 550$ nm). With an improved system (Figs. 11–13 show the setup used at Meudon up to March 1997 using a 1.2 x 1.8 m bench), the observations (on the Sun but also on Jupiter, Mars and the Moon) were also carried in 1996/1997 (we largely improved the stabilities and contrasts — over 50% gain — though not yet to the laboratory values). The initial alignment was still obtained with a collimating mirror but the constraining alignment on a star was eased by a pre-alignment on a pseudo point-source, a laser diode installed 200 m away on the top of the Meudon Solar Tower. With this system, the fine adjustment of the reference aperture stops using the star (still necessary because of the laser diode finite size) is made in a matter of minutes rather than hours... Beside stabilities and contrast measurements, these observations allowed to test the dual filtering: large field, 30" or more, at telescope level for the scientific field-of-view, and reduced field-of-view, a fraction of the resolution, in the reference interferometer where the phase (cophasing control) is measured.

At this point, the major demonstration is made: we observed and cophased fringes on the Sun and we are convinced that our major difficulties are linked to the lack of fine pointing (seeing is bad at Meudon, small fields are not always superimposed, and the small size of the refractor is

sensitive to scintillation when observing stars). Accordingly, by September 1997, the system will be upgraded to three telescopes, and fine pointing (active mirrors) will be implemented

7. THE 3-TELESCOPE IMAGING BREADBOARD

Fig. 14 shows the optical layout of the 3-Telescope Imaging Breadboard which is currently integrated at Verrières on a large optical bench (1.5 x 3 m) before being moved to Meudon for further observations. This new breadboard will also use the small 60 mm refractors (cf. Fig. 13) to simulate the entrance telescopes and, alike the experiment carried in laboratory in 1995, a collimator (8 inches Celestron), will be used to illuminate the objectives during the integration and testing phase. New hardware and software will be implemented for the 3-Telescope Imaging Breadboard financed on one side by CNES R & T funds and, on the other, by ESA Contract Optical Aperture Synthesis Technologies 2 (OAST2). In particular, a second delay line and 3 active mirrors have been provisioned that can be controlled up to 100 Hz.

Fig. 11 - The 2-Telescope Breadboard of the Solar Interferometer at the "Grand Sidérostat de Foucault" at Meudon Observatory in March 1997.

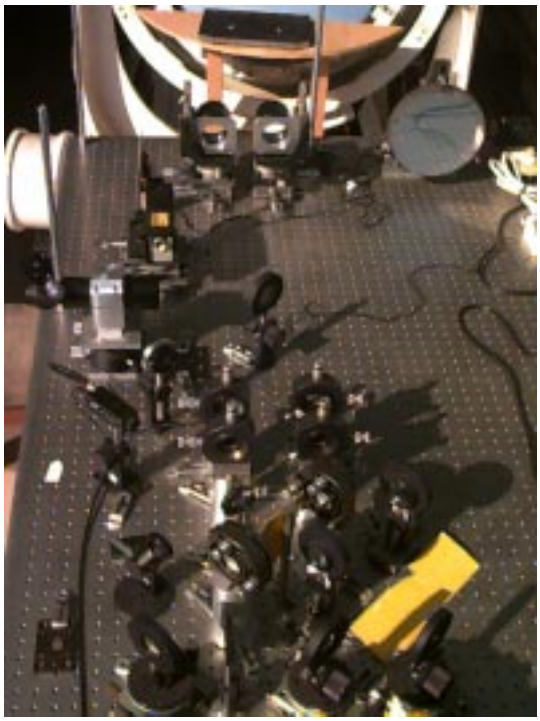

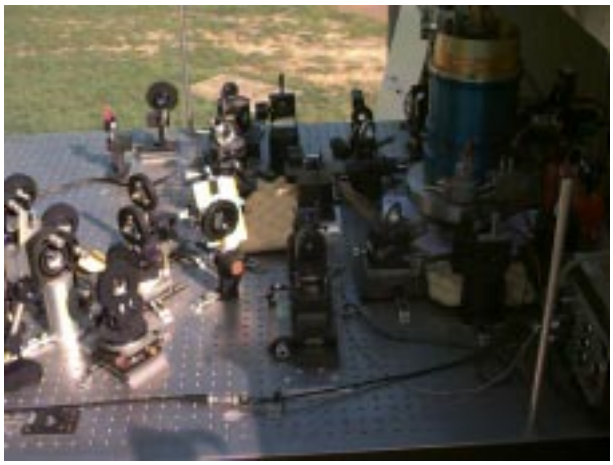

Fig. 12 - Top and side views of the 2-Telescope Breadboard at Meudon Observatory in March 1997.

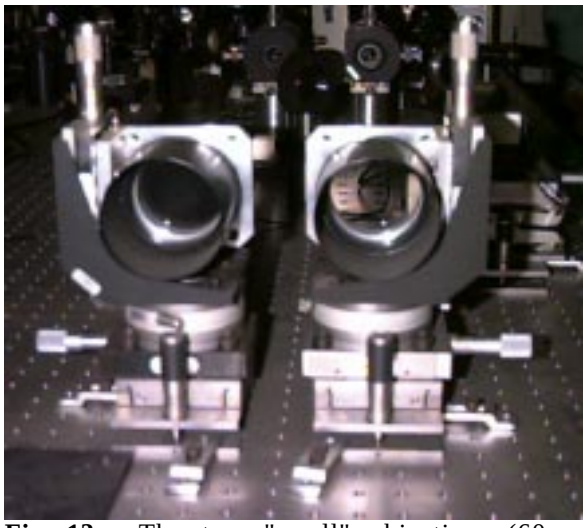

Fig. 13 - The two "small" objectives (60 mm diameter) which simulate the entrance telescopes of the 2-Telescope Breadboard.

With the 3-Telescope Breadboard we will apprehend the system aspects of multiple telescopes control and imaging. Control can either be achieved by a cascade of servo-control with strictly similar reference interferometers (the method that we favor) or with some more complexity by a triple modulation and closure phase technique when associating 3 telescopes together. The 3-Telescope Breadboard will allow to investigate the performances of the two methods. However, we lack of an appropriate CCD camera to fully qualify the different imaging approaches (phase closure for low flux or high rate acquisitions, *etc*.). It would be a plus for the performances evaluation to acquire a reliable CCD system for the ground system. This has been asked to INSU in France.

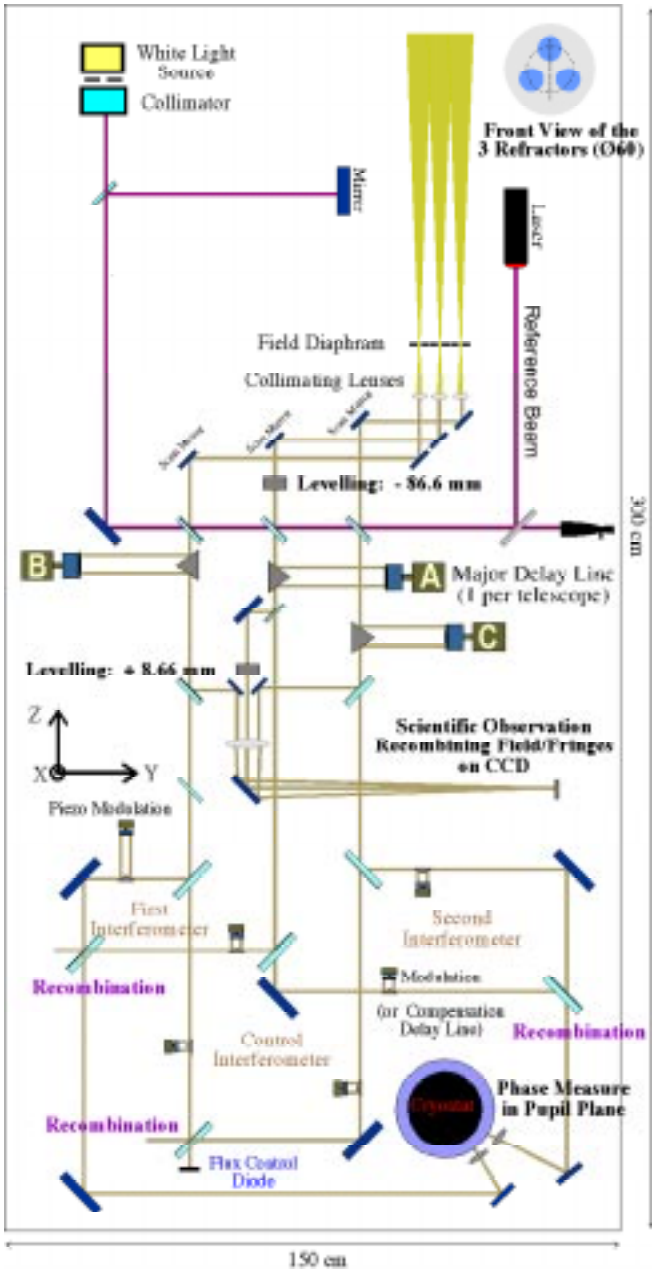

Fig. 14 - Schematic layout design of the 3-Telescopes breadboard as it is currently implemented on our new 1.5 x 3 m optical table. Note that by applying the corrective error signal to Delay Line "A" rather than "B", one can switch from the "cascading" mode of interferometers control ("B" servo-controlled on "A" and "C" on "B") to the "simultaneous" mode ("A" and "C" servo-controlled on "B"). Note also the 3 Active Mirrors and the new imaging channel where the 3 beams are recombined.

8. APPLICATION TO THEMIS

5-Segment Pupil

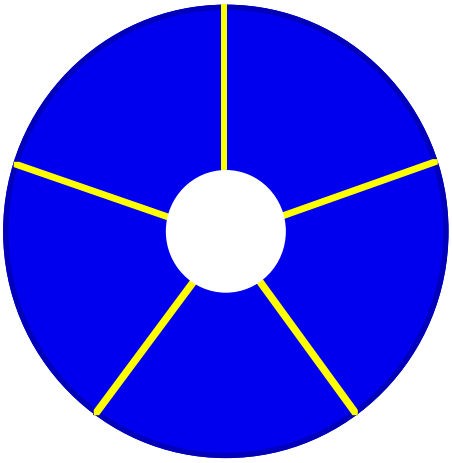

7-Segment Pupil

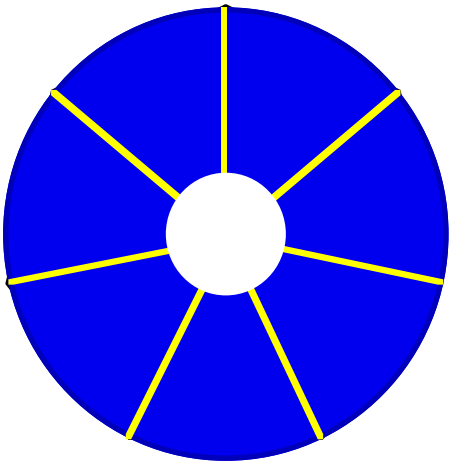

The application to ground-based solar astrophysics is direct. The cophasing method is working in the visible on any diaphragmed field on the Sun. It is, then, directly applicable to THEMIS. With access to the THEMIS pupil at the level of the present Active Mirror, we can envisage replacing this simple system by a 7 pupil's segments cophased pupil (7 reference interferometers) helped by 7 active mirrors (one per subpupil). Our current control application (COPHASE), based on Windows NT 4.0, is already dimensioned to control 7 reference interferometers as well as the pointing of 7 active mirrors.

Fig. 15 - Application to THEMIS of the Cophased Interferometry approach of SOLARNET. Because the THEMIS pupil is already a full pupil (no need to add telescopes) the proper choice is to use the full pupil and consider individual segments as the entrance subpupils to be cophased. Optimum THEMIS 90 cm telescope are 5 or 7 segments in order to account for an r_0 of 40 to 50 cm or so. Note that direct cophasing interferometry is much more efficient that adaptive optics since the method has been proved to work on extended objects and also since only 6 phase measurements (6 reference interferometers) and, then, 6 servo-controlled delay lines are required to phase the whole pupil.

The prospects are therefore excellent to achieve, permanently, 0.1 arcsec spatial resolution without back effects (since the pupil is full all observing modes, dispersed spectra or spectro-imaging, are allowed) with THEMIS in the near future. It is our intention to propose an interferometric mode for Permanent High Resolution Observations for the second generation of THEMIS instrumentation.

9. CONCLUSION

We have developed a complete design for a solar interferometer suitable to represent a major breakthrough in the Solar Physics findings of the next century. We proved that the major assumption of the overall concept, the cophasing of the array, is feasible and, moreover, that performances to expect are very high. We are working on a 3-Telescope Breadboard, cophased and pointed, which will, by September 1997, demonstrate the system aspects and show the first interferometric images of the Sun made with independent telescopes. With continuous observations of the Sun with 0.1" spatial resolution on a 40" FOV, a breakthrough will be achieved in Solar Physics on ground if this system is implemented in THEMIS (instruments of second generation). More details on the instruments (on ground and in Space), cophasing techniques, image reconstruction algorithms and performances, double monochromator design (focal instrument of the Space's programmes), and our laboratory and "sky" results are available on our web server: http://must.aerov.jussieu.fr.

Acknowledgments. We are grateful to MATRA MARCONI SPACE for financial support in 94 and 95 that allowed to complete the 2-Telescope Breadboard and to carry the solar tests at

Meudon Observatory. This work is supported by CNES R & T Grants since 92. ESA Contract OAST2 is supporting most of the evolution of the Breadboard from 2- to 3-Telescope.

10. REFERENCES

Coradini, M., Damé, L. et al.: 1991, "Solar, Solar System and Stellar Interferometric Mission for Ultrahigh Resolution Imaging and Spectroscopy (SIMURIS)", Scientific and Technical Study — Phase I, ESA Report SCI(91)7

Damé, L.: 1997, "A Revolutionary Concept for High Resolution Solar Physics: Solar Interferometry", ESA Symposium on *Scientific Satellites Achievements and Prospects in Europe*, Paris, France, 20–22 November 1996, (Proc. to be published by the AAAF)

Damé, L. et al.: 1997, "Solar and Planetary High Resolution UV Imaging by Interferometry, SOLARNET", Proposal submitted to ESA Opportunity Call SP-1201, December 1996, for "Externally Mounted Payloads during the Early Space Station Utilisation Period"

Damé, L.: 1996, "The MUST/3T Solar Interferometer: An Interferometric Technologies TestBed on the International Space Station", ESA Symp. on *Space Station Utilization*, Darmstadt, 30 Sept.–2 Oct. 1996, Ed. T.D. Guyenne, ESA SP-**385**, 369

Damé, L., Derrien, M., Kozlowski, M., Antonucci, E., Ragazzoni, R. and Tondello, G.: 1996, "SIMURIS: a UV and XUV Mission for High Resolution Solar Physics", *Advances in Space Research*, **17**(4/5), 377–380

Damé, L., Derrien, M., Kozlowski, M., Ruilier, C., Appourchaux, T. and David, F.: 1995a (September), "Observation Directe et Asservissement des Franges avec un Interféromètre Solaire à Deux Télescopes au Grand Sidérostat de Foucault à l'Observatoire de Meudon", Rapport Interne du Service d'Aéronomie, v1.0

Damé, L., Derrien, M., Kozlowski, M. and Ruilier, C.: 1995b, "Instrumental Prospects in Solar Interferometric Imaging", JOSO 27th Annual Meeting, Benesov, Tcheque Republic, 12–15 November 1995, *JOSO Annual Report* **1995**, 52-59

Damé, L.: 1994, "Solar Interferometry: Space and Ground Prospects", in *Amplitude and Intensity Spatial Interferometry II*, Ed. J.B. Breckinridge, Proc. SPIE–**2200**, 35–50

Damé, L., Derrien, M. et Kozlowski, M. : 1994 (September), "Démonstration de Faisabilité de l'Interférométrie Spatiale Solaire par Asservissement Synchrone sur les Franges en Lumière Blanche", Rapport Interne du Service d'Aéronomie, v1.0

Damé, L.: 1993: "Actively Cophased Interferometry with SUN/SIMURIS", in *Spaceborne Interferometry*, Ed. R.D. Reasenberg, Orlando, Proc. SPIE–**1947**, 161

Damé, L. et al.: 1993a, "A Solar Interferometric Mission for Ultrahigh Resolution Imaging and Spectroscopy (SIMURIS)", Proposal to ESA Call for the "Next Medium Size Mission — M3"

Damé, L., Martić, M. and Rutten, R.J.: 1993b, "Prospects for Very-High-Resolution Solar Physics with the SIMURIS Interferometric Mission", in *Scientific Requirements for Future Solar Physics Space Missions*, Oslo, 12-13 January 1993, Ed. B. Battrick, ESA SP-**1157**, 119–144

Damé, L., 1992: "Demonstration and Performances of Real-Time Fringe Tracking: a Step Towards Cophased Interferometers", in *Solar Physics and Astrophysics at Interferometric Resolution*, Eds. L. Damé and T.D. Guyenne, ESA SP–**344**, 277

Damé, L. and Martić, M.: 1992, "Study of an Optimized Configuration for Interferometric Imaging of Complex and Extended Solar Structures", in *Targets for Space Based Interferometry*, Ed. C. Mattok, Baulieu, ESA SP–**354,** 201

Damé, L. and Rutten, R.J.: 1992, "Prospects with SIMURIS", in *Solar Physics and Astrophysics at Interferometric Resolution*, Eds. L. Damé and T.D. Guyenne, ESA SP–**344**, 21

Damé, L., et al.: 1992, "Design Rationale of the Solar Ultraviolet Network (SUN)", ESO Conference on *High Resolution Imaging by Interferometry II*, Garching 15-18 October 1991, Eds. J.M. Beckers and F. Merkle, ESO Conference and Workshop Proceedings **39**, 995

Damé, L., et al.: 1989, "A Solar Interferometric Mission for Ultrahigh Resolution Imaging and Spectroscopy (SIMURIS)", Proposal to ESA for the "Next Medium Size Mission — M2"